

AN INTERESTING FALL-OUT OF HIGH-ENERGY PHYSICS TECHNIQUES:  
THE IMAGING OF X-RAYS AT VARIOUS ENERGIES FOR BIOMEDICAL APPLICATIONS

G. Charpak and F. Sauli  
CERN, Geneva, Switzerland

Presented by

F. Sauli at the Conference on Computer Assisted Scanning,  
Padova, Italy, 21-24 April, 1976

and by

G. Charpak at the Topical Meeting on Intermediate Energy Physics,  
Zuoz, Switzerland, 31 March-10 April, 1976



## 1. INTRODUCTION

Multiwire proportional chambers (MWPC) and drift chambers are now a widespread technique in high-energy physics and nuclear physics.

The first studies in the properties of multiwire chambers<sup>1,2)</sup> revealed the following features which are essential for the imaging of neutral radiations:

- Self triggering.
- Two-dimensional read-out. The secondary radiation produced by  $\gamma$  or neutrons is usually of a small energy and cannot cross several chambers. The read-out of the avalanche position along the wire was shown to be possible using the signal induced on cathode elements perpendicular to the anode wires.
- The electrons liberated in drift spaces attached to a chamber are easily transferred to the proportional chambers. This opens the way to different methods of increased efficiency, by conversion, in appropriate drift spaces, of the neutral radiation.

In the last few years the work of a rather limited number of groups has shown that indeed powerful tools can thus be designed for a variety of applications. Large surface two-dimensional detectors sensitive to X-rays of energies ranging from a few keV to some tens of keV can revolutionize traditional techniques of X-ray diffraction studies of molecular structure.

Detectors sensitive in the region of a few tens of keV to about 1 MeV have a range of applications in nuclear medicine, permitting imaging of the radiation emitted by radio-isotopes injected into living bodies. Very powerful techniques, based on scintillators coupled to photomultipliers or image intensifiers, exist in this field, and the multiwire chambers may offer advantages only in some limited cases. It is, however, clear that they are very promising in some fields where large areas incompatible with scintillators are required, or where their great spatial accuracy is required. Large-area, position-sensitive, slow neutron detectors offer considerable applications in the expanding field of molecular structure studies with monochromatic neutrons of wavelength larger than  $2 \text{ \AA}$ .

We are convinced that high-energy or nuclear physicists, familiar with the construction of large systems of multiwire chambers and with mass data handling, are in a good position to contribute to fruitful developments by entering into adventures of multidisciplinary projects using these takings.

We will discuss some examples of such undertakings.

## 2. THE READ-OUT METHODS

We will not discuss the comparative merits of the different methods of two-dimensional read-out. Some of them make use of analogical methods which are patented. Although most of the time of dubious validity because of a rather deliberate ignorance of similar work in connected fields or on other continents, these patents had the advantage of encouraging some groups to develop their methods to the ultimate possible quality. It is sometimes a matter of taste for the user to adopt one method or the other, but also a matter of physical constraints. The basic fact underlying these methods is that the signal induced in the cathodes by the motion of the positive ions in the regions of an intense electric field close to the anode wires is centred on the avalanche<sup>2)</sup>.

The measurement of the centroid of these avalanches can be done by using delay lines where the induced signal is injected at variable positions, various charge division methods, direct computing of the centroid of the charges, or digital methods similar to those used to read out the anode wires.

A review of the first analog read-out methods used in MWPC and their relations to similar techniques used in spark chambers can be found elsewhere<sup>3,4)</sup>.

A precise critical review of the most recent applications of the delay line and current division methods has been made<sup>5,6)</sup>. The conclusions of this analysis are the following.

Position sensing with delay lines requires a smaller signal than charge division methods for equal relative resolutions; with capacitive coupling to a delay line, the method popularized by the Perez-Mendez group<sup>7)</sup>, a substantial attenuation of the signal occurs which may result in a loss of accuracy.

Several examples of construction where the delay lines are directly coupled to the electrodes or part of the electrodes can be found in the literature<sup>8-12)</sup>; these few references are only given as examples of various approaches. With resistive electrodes the choice can be made between charge division and the time dispersion method, i.e. change of the rise-time as the signal propagates along a resistive line<sup>13)</sup>; the former is several times faster.

However, none of these methods is universal and in some cases physical constraints may impose one solution. Such an example can be found in the slow neutron detector described by Alberi et al.<sup>14)</sup>.

## 3. THE IMAGING OF X-RAYS OR $\gamma$ -RAYS

Two important problems dominate the design of chambers intended to measure the spatial distribution of X-rays: the efficiency and the accuracy.

The efficiency of gaseous absorption drops rapidly with energy; at high energies solid converting materials inside drift chambers are a possible solution.

The accuracy is sometimes limited by the intrinsic avalanche localization accuracy of the chambers, which can be as good as  $\sigma \sim 50 \mu\text{m}$ , but in most of the cases it is limited by two other factors: the range in the gas of the secondary electron ejected by photoelectric or Compton effect, and the escape X-rays following a photoelectric effect, which give rise to several avalanches separated by large distances<sup>15)</sup>. These effects can also, to a large extent, be cured with narrow channel converters in drift spaces, limiting the range of electrons. This leads to very different mechanical chamber configurations according to the energy of the X-ray sources.

### 3.1 Imaging of soft X-rays (5 keV to about 50 keV)

We will overlook the domain of ultrasoft X-ray imaging (0.1 to 6 keV), important in astronomy. Such counters can be used as image detectors in the focal plane of grazing-incidence telescopes, for X-ray astronomy applications<sup>16)</sup>.

Above 5 keV and up to a few tens of keV a very important domain is the one connected to the structure analysis using X-ray diffraction. The study of protein structures using protein crystals is one of the most promising in this field. The replacement of photographic films as X-ray detectors or of small counter scanning methods offers the possibility of gains by factors of 100 or 1000 in the time so far necessary to obtain the data on molecular structure. New domains such as rapid variation of structures can be opened by these techniques.

Figure 1 shows the mean free path for absorption of X-rays in several noble gases as a function of energy, at atmospheric pressure; the X-ray intensity after traversing a thickness  $\ell$  is given by  $I = I_0 e^{-\ell/\lambda}$  and the efficiency of conversion is  $1 - e^{-\ell/\lambda}$ .

We see clearly that to obtain efficiencies close to 100% we have to go to heavy gases and to large thicknesses well above 1 cm, or to high pressures. Large thicknesses are a nuisance because of the degradation of the accuracy for inclined tracks, as shown in Fig. 2; directions inclined with respect to the chambers give rise to elongated images. This has led for instance Cork et al.<sup>17,18)</sup> to the construction of 8 mm thick chambers with a high pressure of xenon (5 atm).

At CERN we have been led to another solution under the incentive requirements of two groups: R. Mössbauer, who needs imaging chambers for 20 keV X-rays, and a Paris group using the synchrotron radiation emitted by the electron storage rings at Orsay. Electron storage rings are modern, powerful sources of X-rays with the following characteristics:

- The spectrum is continuous and very intense. With curved crystals a narrow bandwidth ( $\sim 2 \text{ eV}$ ) can be selected between 0.5 and 3 Å (25 keV to 4 keV) which is an ideal wavelength for crystalized protein structures. The intensity in such a narrow

bandwidth is  $10^3$  higher than that obtained with a standard sealed copper X-ray tube. A realistic evaluation of the running conditions leads to average fluxes of diffracted photons, by small protein crystals, of  $10^6$ /sec.

- The beam geometry is very good. The divergence is  $\sim 1$  minute of arc in the vertical plane and 3 minutes of arc in the horizontal plane. So long crystal-to-detectors distances are possible, which is very important for crystals with large cells.
- The tunability of the source is a very powerful tool, since one can play with the wavelength below and above K edges of the elements composing the sample.

To make a full use of the qualities of the synchrotron radiation, it appeared that MWPCs offer ideal properties, both in terms of accuracy and rate capability. To circumvent the source of error due to the converter volume thickness (see Fig. 2), conversion and drift spaces having spherical symmetry have been developed<sup>19)</sup>. We describe here the preliminary results obtained in a large prototype spherical drift chamber<sup>20)</sup>. On one side of a conventional bi-dimensional imaging MWPC a gaseous conversion volume is mounted in which a suitable set of electrodes maintains an electric field with radial symmetry, its centre being the foreseen crystal position (Fig. 3). The upper electrode consists of a thin, gas-tight aluminium cap, while the lower spherical electrode is a thin grid to let the primary charge, produced in the drift space by photoelectric conversion, smoothly drift to the lower imaging chamber. The chamber we have operated has a 10 cm thick radial drift space and an acceptance of  $90^\circ$  (or 1.8 sr); the underlying MWPC has an active area of  $50 \times 50$  cm<sup>2</sup> and 2 mm anode wire spacing. Use of the data in Fig. 1 allows us to compute the efficiency for 8 keV X-rays in argon (84%) and in xenon (100%).

For the imaging, we have used the method of measuring the centre of gravity of the induced positive signals on the cathodes in an analog way.

One of the apparently surprising results is the fact that the accuracy of the chamber, measured with a collimated beam of 8 keV X-rays, is better than 700  $\mu$ m (FWHM) in all directions, while it should, in the direction of the anode wire, be equivalent to their spacing (2 mm). What happens is that the originally very localized primary charge, due to diffusion during the drift, reaches a size between 1 mm and 2 mm, and the energy is split between two adjacent wires thus resulting in a precise determination of the centroid of the charge distribution between the wires.

This is very rewarding since, from our experience, chambers with 1 mm wire spacing and 50 cm length are difficult to operate while 2 mm spacing is compatible with sizes of several square metres as we have learned it from our practice in high-energy physics.

The possibility of operating large surfaces is also connected with the possibility of using spherical drift spaces of large size (up to 50 cm for instance) which in many cases would eliminate the need to use xenon as a component of the filling gases.

At higher X-ray energies, the accuracy of a chamber is limited by the range of the photoelectrons, which at 20 keV is of the order of 1 mm in an argon-filled chamber. In a xenon-filled chamber instead, the range is 1 mm around 40 keV; we may thus consider these energies as practical upper limits for chambers at atmospheric pressures, if the intrinsic localization accuracy has to be maintained.

Examples of X-ray diffraction patterns in a smaller spherical drift chamber have already been published<sup>19)</sup>. Here we would like to stress the fact that the chamber can be used as an X-ray pinhole camera, by placing its focal plane on absorber with a small hole in the centre. Figure 4 shows the image obtained of letters traced with a radioactive solution on a support.

Another field of application of this kind of detector is the structural study of muscular tissues. In certain conditions, muscle fibres form a regular pattern of large molecules, somehow similar to a crystal; characteristic diffraction patterns can be produced that are sensitive to spacings down to few tens of Å. The study could be static or, if the data acquisition rate is high enough, dynamic<sup>21)</sup>. Figure 5 (from Ref. 21) shows a rat tail collagen unidimensional pattern obtained with 10 keV X-rays.

### 3.2 Imaging of intermediate energy X-rays (40 keV to about 100 keV)

This is a very important field in nuclear medicine. The imaging is here obtained by the injection of radioactive tracers; the most commonly used are:

$^{125}\text{I}$	period 60 days,	$\gamma$ of 35 keV	(7% of total activity)
$^{197}\text{Hg}$	" 65 hours,	$\gamma$ of 77 keV	(18%)
$^{195}\text{Au}$	" 120 days,	$\gamma$ of 99 keV	(10%)
$^{133}\text{Xe}$	" 5 days,	$\gamma$ of 81 keV	(37%)
$^{99}\text{Tc}$	" 6 hours,	$\gamma$ of 140 keV	(90%)

The last isotope,  $^{99}\text{Tc}$ , is the more convenient since it is easily separable from the parent, longer-lived  $^{99}\text{Mo}$ . Both for obtaining high efficiencies and a short range of the photoelectron, high-pressure xenon chambers have been used in this range of energies. With a 6 cm thick MWPC, filled with Xe-CO<sub>2</sub> at 4 atm, Kaufman et al.<sup>22)</sup> could obtain efficiencies around 20% for 100 keV photons, with accuracies in the millimetre range. This has to be compared with the scintillation cameras which now yield accuracies of about 5 mm, with efficiency close to 100% and a good energy resolution. We thus see that the interest of the MWPC systems

can either be in cases where a very high accuracy is wanted and where the dose limitation is not relevant, in dynamical studies in animals or in cases where sizes incompatible with the scintillation cameras (at most  $32 \times 32 \text{ cm}^2$ ) are required. However, the drift chambers with high density offer, in some cases, an elegant way of overcoming the difficulty (see below).

### 3.3 Imaging of $\gamma$ -rays between 100 keV and 1 MeV

Solid converters can be placed inside a drift space, serving two separate purposes: to increase the efficiency of  $\gamma$ -conversion and to limit the range of secondary electrons to narrow, well-defined channels.

Two examples of realization of such converters have been described: one at Berkeley<sup>23-25</sup>, the other one at CERN<sup>26,27</sup>). In the first approach the converter consists of layers of lead honeycomb; each layer is electrically isolated from the other and a drift field is applied between them to extract the ionization electrons liberated in the gas by the conversion electrons. The lead honeycomb is characterized by a lead thickness of 70  $\mu\text{m}$  on the lateral walls, an aperture of 3 mm in the honeycomb cell, and a thickness of 3 mm of the honeycomb layer. The efficiency of detection of 500 keV  $\gamma$  is of the order of 2.5% for a single layer, and the accuracy 6 mm FWHM. The approach at CERN has been different (Fig. 6, from Ref. 26); grids of lead-bismuth with 1 mm apertures, 0.5 mm thickness, and 1.5 mm pitch are isolated from each other with a potential across the grid producing the electric drift field inside the channels. The accuracy obtained is 1.3 mm (FWHM) at 0.6 MeV with an efficiency of about 5% per layer of 1 cm.

Further improvement in this direction has lead Jeavons to 20% efficiency at 0.5 MeV<sup>27</sup>). These developments are of importance for positron imaging.

Because the two  $\gamma$ -rays emitted by the annihilation of positrons are at  $180^\circ$ , collimators are not necessary to determine activity distributions in space if the two opposite photons are detected in coincidence.

Very active positron-emitting isotopes exist of the atoms that mainly compose the living tissues, as shown in Table 1.

This has lead some laboratories to equip themselves with accelerators aimed only at the production of these isotopes.

The initial *in vivo* results of the Perez-Mendez group illustrate the great potential possibilities of the positron MWPC camera; the intrinsic resolution of a live  $^{64}\text{Cu}$  positron emitter embedded in 10 cm of lucite is shown in Fig. 7; the resolution is 7 mm FWHM. Figure 8 shows images of a dog labelled with  $^{18}\text{F}$ .

The results obtained at CERN show that even greater accuracies and efficiencies can be obtained; the accuracy is, of course, limited by the range of the positron in the living tissues, which is in general of a few millimetres (Table 1).



Table 1

Some data on some interesting short-lived accelerator-produced positron emitters

Nuclide	Half life (min)	Positron energy (MeV)		Range (mm)	
		Mean	Max	Mean	Max
$^{11}\text{C}$	20.4	0.38	0.96	1.2	4.1
$^{13}\text{N}$	10.0	0.48	1.20	1.7	5.4
$^{15}\text{O}$	2.1	0.70	1.74	2.8	8.2
$^{18}\text{F}$	11.0	0.26	0.66	0.7	2.5

Jeavons and Cate<sup>27)</sup> report some calculations on the optimum converter structure which is a function of the  $\gamma$ -ray energy; however one should keep in mind that the diffusion of electrons in the gas inside the channels sets a practical limit to the channel diameter. If a hole is 100  $\mu\text{m}$  wide and the diffusion is 0.5 mm per cm of drift, only a few percent of the electrons liberated in the gas will drift to the exit before being captured by the walls. Holes of 1 mm<sup>26)</sup> seem a more reasonable size. Experiments with glass tubes<sup>25,26)</sup>, much easier to construct, show that they are a possible solution for cheap, large-scale construction. Their main drawback, which is in the charging up of the surface, has been to some extent cured in the channel plate multipliers.

Similar research is being pursued in several laboratories. The advantage of the MWPC positron camera over the scintillation camera is in the larger surface attainable at lower cost, in the higher accuracy, and in the higher possible rates of  $10^6/\text{sec}$  and above. The disadvantage is in the absence of energy resolution and in the lower efficiency compared to scintillators.

#### 4. IMAGING OF NEUTRONS

Slow neutrons offer considerable advantages as compared to X-rays in some domains of crystalline structure studies. Whenever wavelengths between 1 and 20  $\text{\AA}$  are needed, the X-rays are strongly absorbed, while the matter is usually transparent to slow neutrons.

Two-dimensional position-sensitive detectors offer for neutrons the same advantages as for X-rays, i.e. higher rates of data collection, possibility to study systems in rapid evolution. The detection medium is specific to the absorption properties of slow neutrons; two filling gases,  $^3\text{He}$  and  $\text{BF}_3$ , are practical for the detection of slow neutrons because of the reaction

REFERENCES

- 1) G. Charpak, R. Bouclier, T. Bressani, J. Favier and Č. Zupančič, Nuclear Instrum. Methods 62, 262 (1968).
- 2) G. Charpak, D. Rahm and M. Steiner, Nuclear Instrum. Methods 80, 13 (1970).
- 3) G. Charpak, Annu. Rev. Nuclear Sci. 20, 195 (1970).
- 4) P. Rice-Evans, Spark, streamer, proportional and drift chambers (Richelieu Press, London, 1974).
- 5) V. Radeka, IEEE Trans. Nuclear Sci. NS21, 51 (1974).
- 6) J.L. Alberi and V. Radeka, IEEE Trans. Nuclear Sci. NS23, 1, 250 (1976).
- 7) R. Grove, I. Ko, B. Keskovar and V. Perez-Mendez, Nuclear Instrum. Methods 99, 381 (1970).
- 8) G. Charpak, R. Bouclier, T. Bressani, J. Favier and Č. Zupančič, Nuclear Instrum. Methods 65, 217 (1968).
- 9) D.M. Lee, S.E. Sobotka and H.A. Thissen, Nuclear Instrum. Methods 104, 179 (1972).
- 10) E. Beardworth, J. Fischer, S. Iwata, M.J. Lévine, V. Radeka and E.E. Thorn, MWPC focal plane detector, BNL 19878 (1975).
- 11) F. Bradamante, S. Conetti, C. Daum, G. Fidecaro, M. Fidecaro, M. Giorgi, A. Penzo, L. Piemontese, A. Prokofiev, M. Renevey, P. Schiavon and A. Vascotto, Proc. Internat. Conf. on Instrumentation for High-Energy Physics, Frascati, 1973 (Lab. Nazionali CNEN, Frascati, 1973), p. 318.
- 12) M. Morgue and R. Chéry, Principes et réalisation d'un compteur proportionnel localisateur de particules, Proc. Internat. Symposium on Nuclear Electronics (Versailles, France 1968), Vol. 1, p. 31.
- 13) C.J. Borkowski and M.R. Kopp, Rev. Sci. Instrum. 46, 951 (1975).
- 14) J. Alberi, J. Fischer, V. Radeka, L.C. Rogers and B. Schoenborn, A two-dimensional position sensitive detector for thermal neutrons, BNL 19487 (1975).
- 15) J.E. Bateman, M.W. Waters and R.E. Jones, RL-75-140 (1975).
- 16) G. Auremia, F. Giovannelli, M. Mastoproprieto and P. Ubertini, Nuclear Instrum. Methods 120, 597 (1974).
- 17) C. Cork, D. Fehr, R. Hamlin, W. Vernon, Nguyen huu Xuong and V. Perez-Mendez, A MWPC as an area detector for protein crystallography, preprint April 1973.
- 18) C. Cork, D. Fehr, R. Hamlin, W. Vernon, Nguyen huu Xuong and V. Perez-Mendez, A high-speed data acquisition system for protein crystallography, Presented by Nguyen huu Xuong at the Internat. Conf. on Computers in Chemical Research, Ljubljana, Zagreb, 1973.
- 19) G. Charpak, Z. Hajduk, A.P. Jeavons, R. Kahn and R.J. Stubbs, Nuclear Instrum. Methods 122, 307 (1974).

- 20) R. Bouclier, G. Charpak, R. Kahn, J.C. Santiard and F. Sauli, Properties of a large-aperture spherical drift chamber, to be published.
- 21) A.R. Farvqi, IEEE Trans. Nuclear Sci. NS22, 5, 2066 (1975).
- 22) L. Kaufman, V. Perez-Mendez and G. Stocker, LBL 1513 (1972).
- 23) C.B. Lim, D. Chu, L. Kaufman, V. Perez-Mendez, R. Hattner and D.C. Price, IEEE Trans. Nuclear Sci. NS21, 6, 388 (1975).
- 24) R.S. Hattner, C.B. Lim, S.J. Swann, L. Kaufman, J.P. Hubercy, D.C. Price, C.B. Wilson, V. Perez-Mendez and D. Chu, IEEE Trans. Nuclear Sci. NS23, 1, 523 (1976).
- 25) D. Chu, K.C. Tam, V. Perez-Mendez, C.B. Lim, D. Lambert and S.N. Kaplan, IEEE Trans. Nuclear Sci. NS23, 1, 634 (1976).
- 26) A.P. Jeavons, G. Charpak and R.J. Stubbs, Nuclear Instrum. Methods 124, 491 (1975).
- 27) A.P. Jeavons and C. Cate, IEEE Trans. Nuclear Sci. NS23, 1, 640 (1976).
- 28) R. Allemand, J. Bourdel, E. Roudaut, P. Convert, K. Ibel, J. Jacobe, J.P. Cotton and B. Farnoux, Nuclear Instrum. Methods 126, 29 (1975).

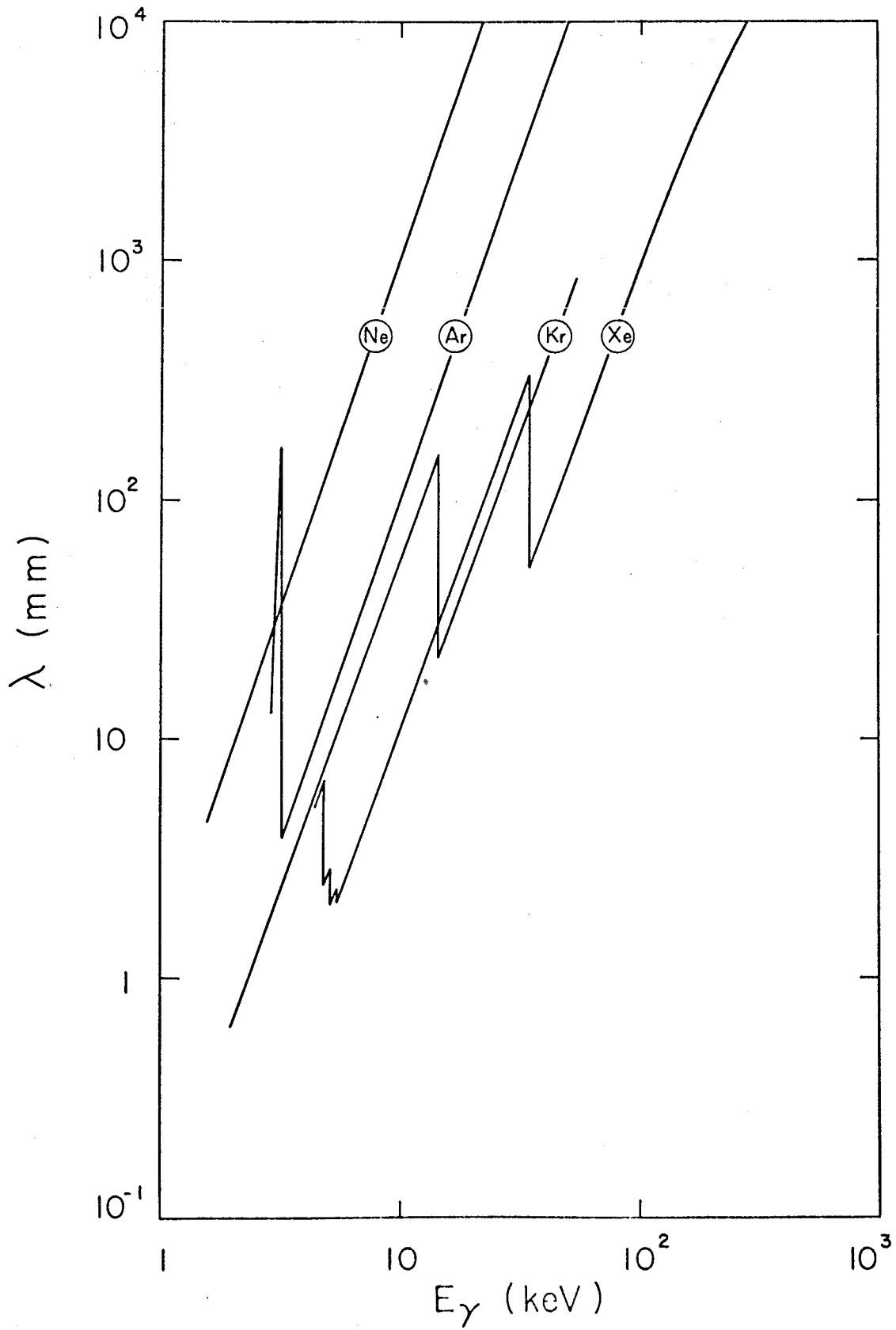


Fig. 1 Mean free path for absorption in several noble gases, at 1 atm

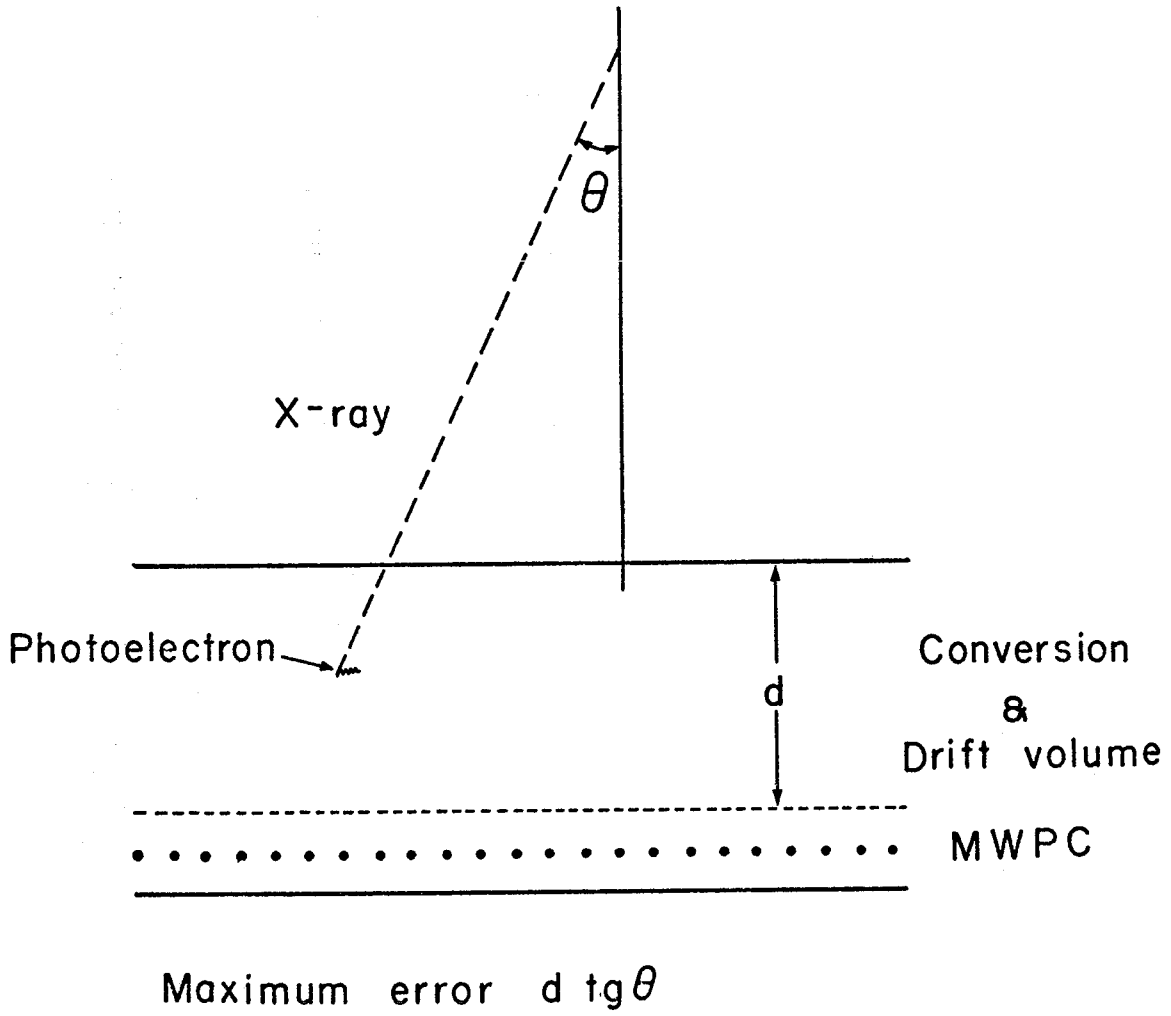


Fig. 2 Source of aberrations in a position-sensitive MWPC with a thick conversion volume

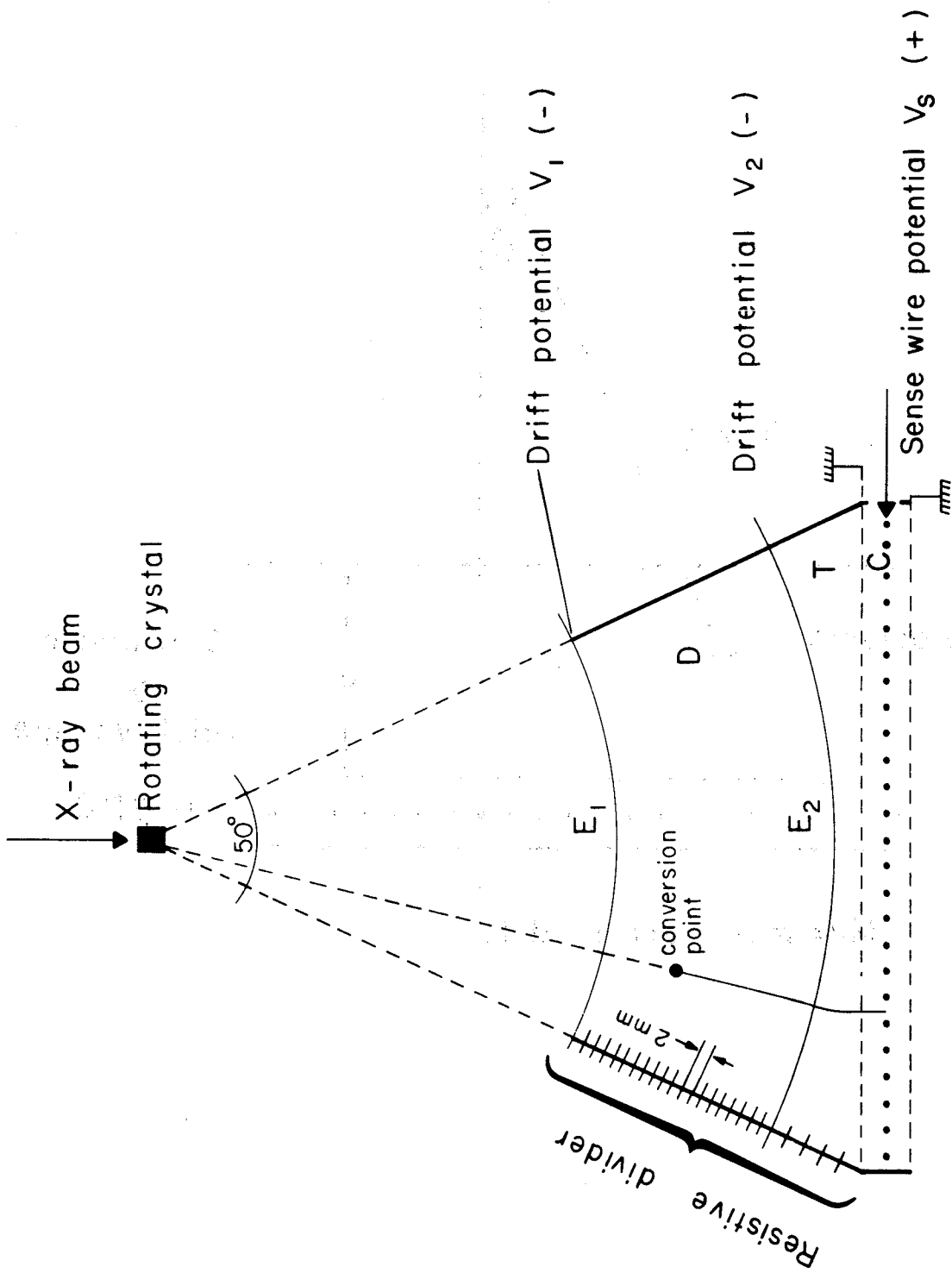


Fig. 3 Schematics of a spherical drift chamber, that corrects the error indicated in the previous figure (from Ref. 19)

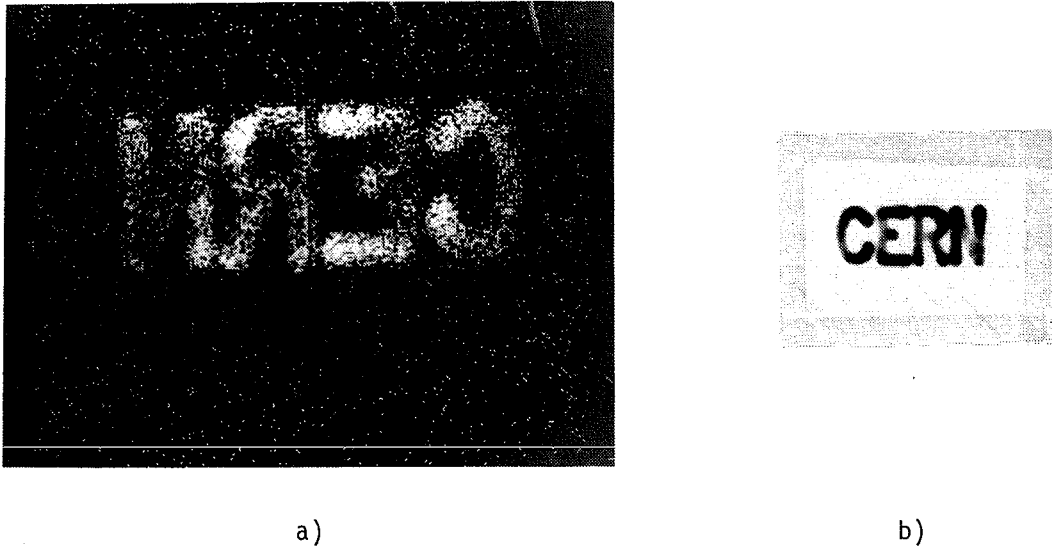


Fig. 4 a) Image obtained with a spherical chamber used as a pin-hole camera, of a radioactive sample writing. The picture on the right (b) shows the autoradiograph of the same sample. Note the correspondence of the non-uniform distribution of activity.

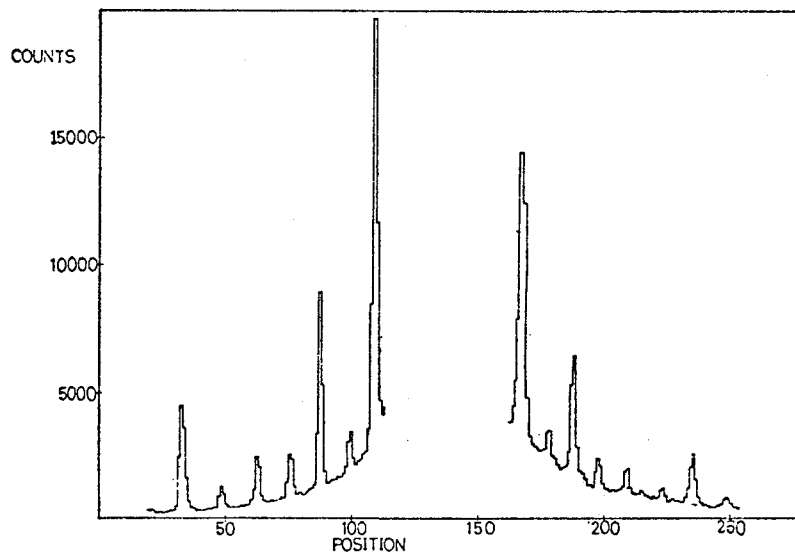


Fig. 5 Rat tail collagen pattern taken on the x-axis of the two-dimensional detector. Sensitivity  $\sim 200 \mu\text{m}$  per channel. (From Ref. 21.)

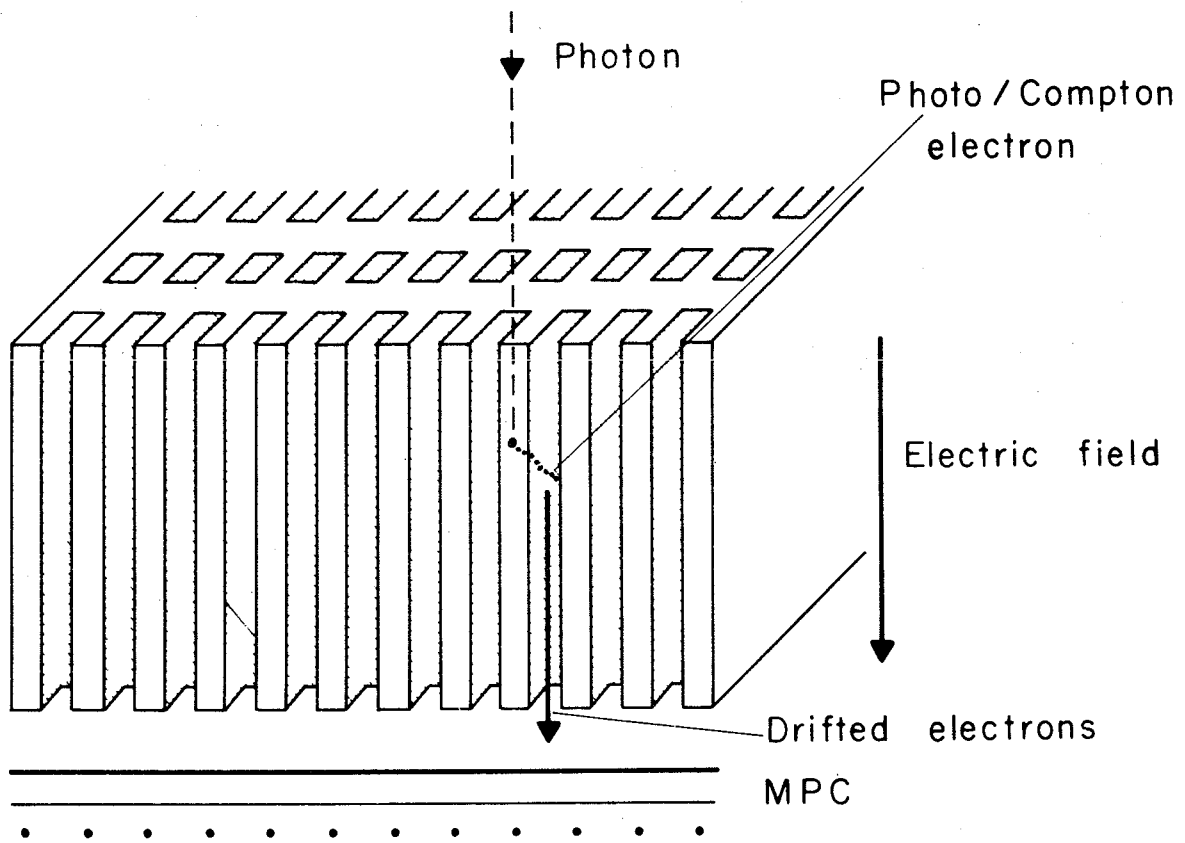


Fig. 6 Schematics of a thick converter and drift volume, composed by a stack of superposed metal layers, with holes forming channels for the drift of extracted electrons to the position sensitive MWPC (from Ref. 26)

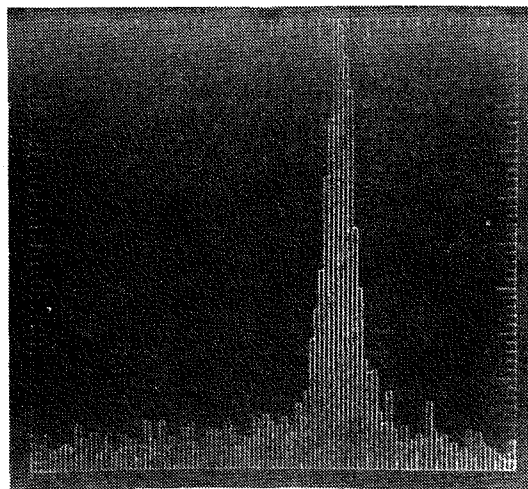


Fig. 7 Space resolution on a line positron emitter, embedded in 10 cm lucite, obtained by Perez-Mendez et al. (Refs. 23-25) with a positron camera



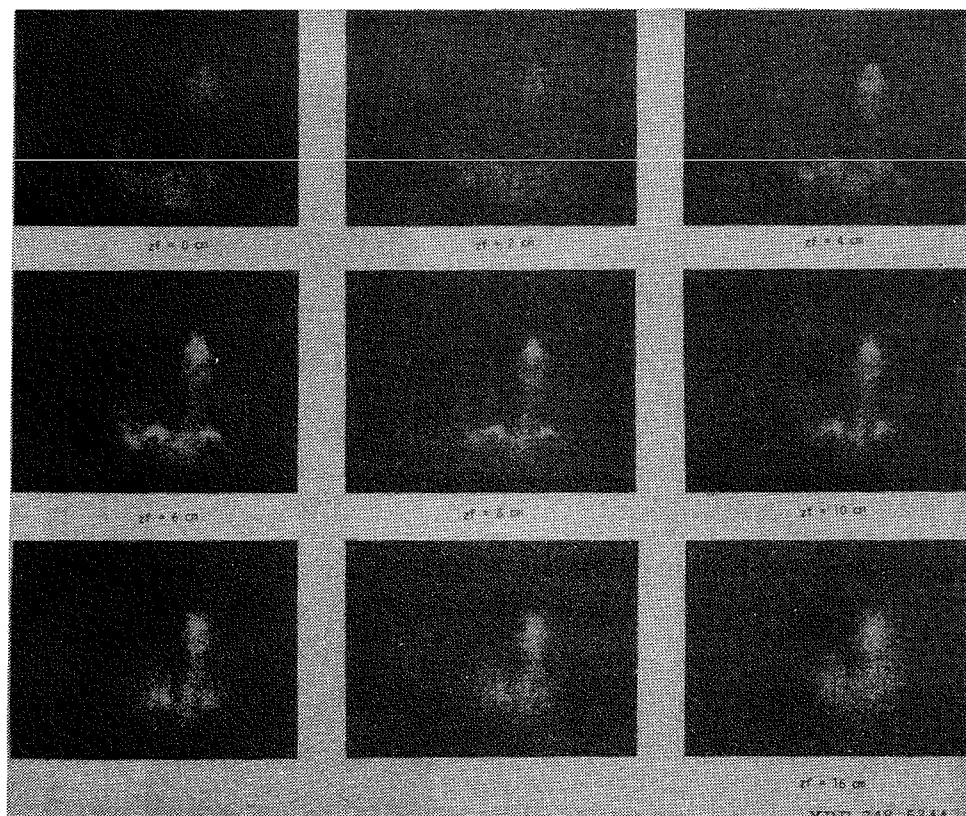


Fig. 8 Tomographic images of a dog labelled with  $^{18}\text{F}$  (from Ref. 25), obtained with a positron imaging system by Perez-Mendez et al.

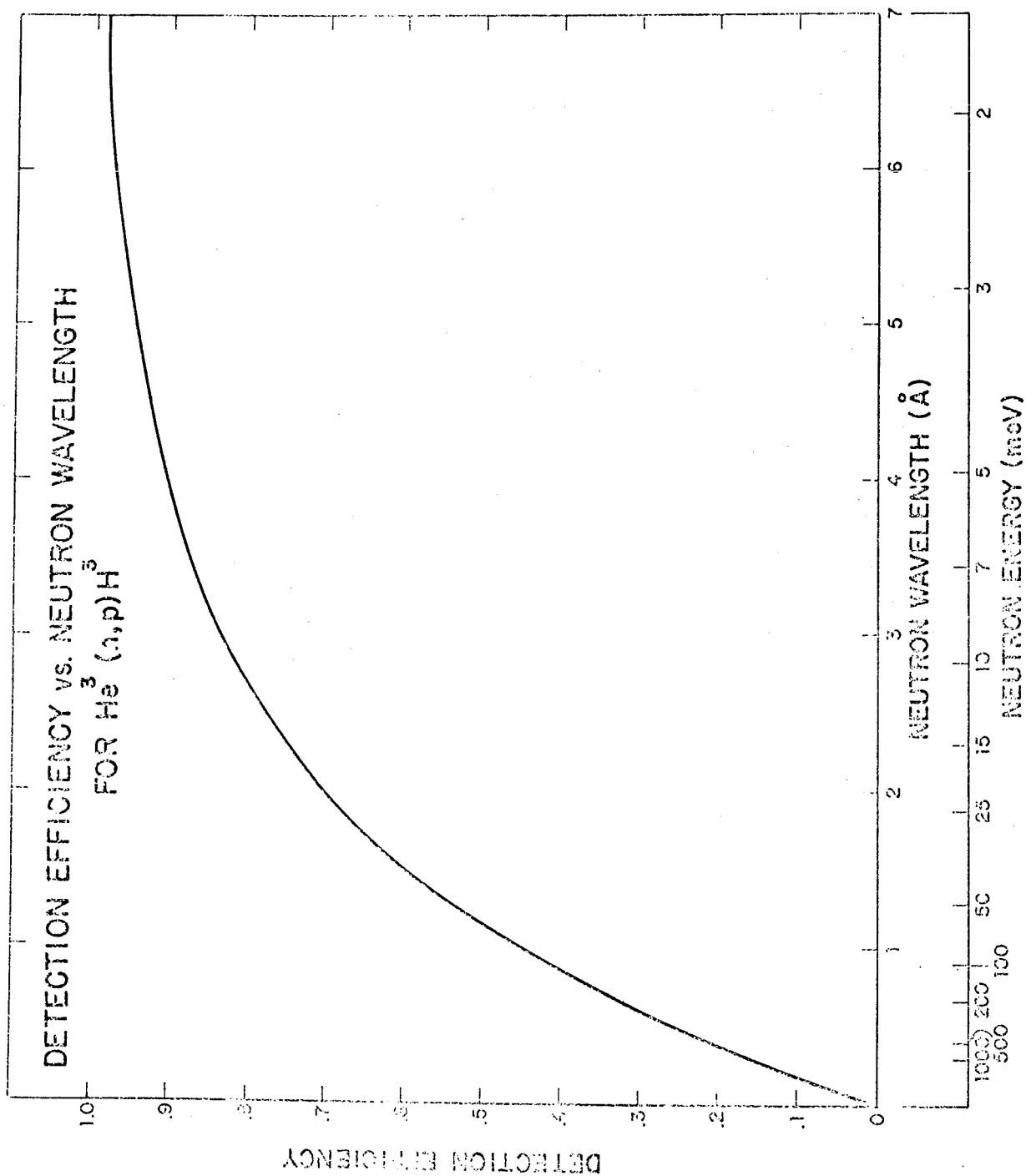


Fig. 9 Efficiency of a slow neutron gaseous detector, versus neutron energy, as obtained by Alberi et al.<sup>14)</sup>

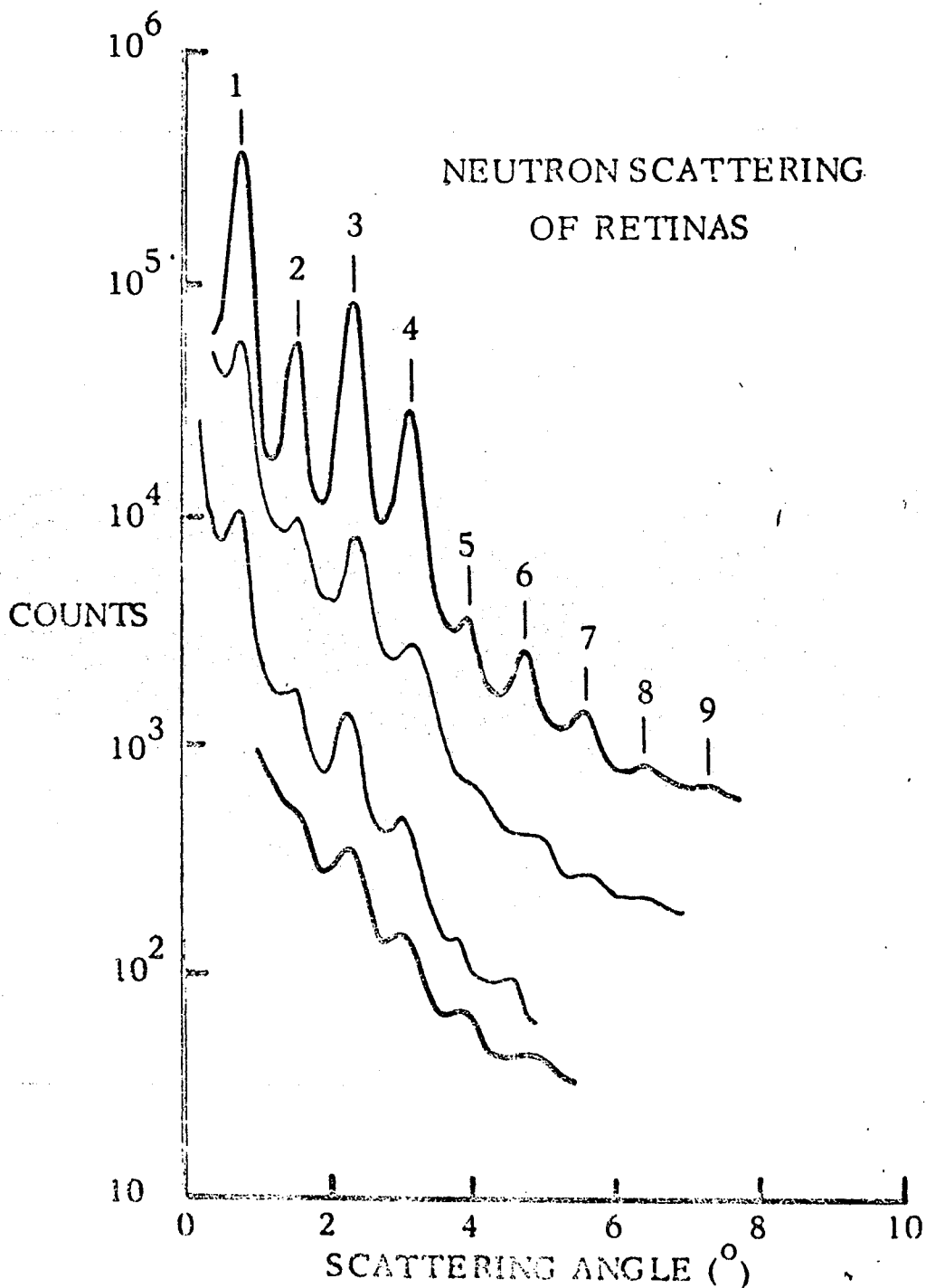


Fig. 10 One-dimensional projection of the scattering of slow neutrons on a retina, showing characteristic pattern (from Ref. 14)

C. IRL (270.404)  
DATE 25-JUN-74 14:51:32

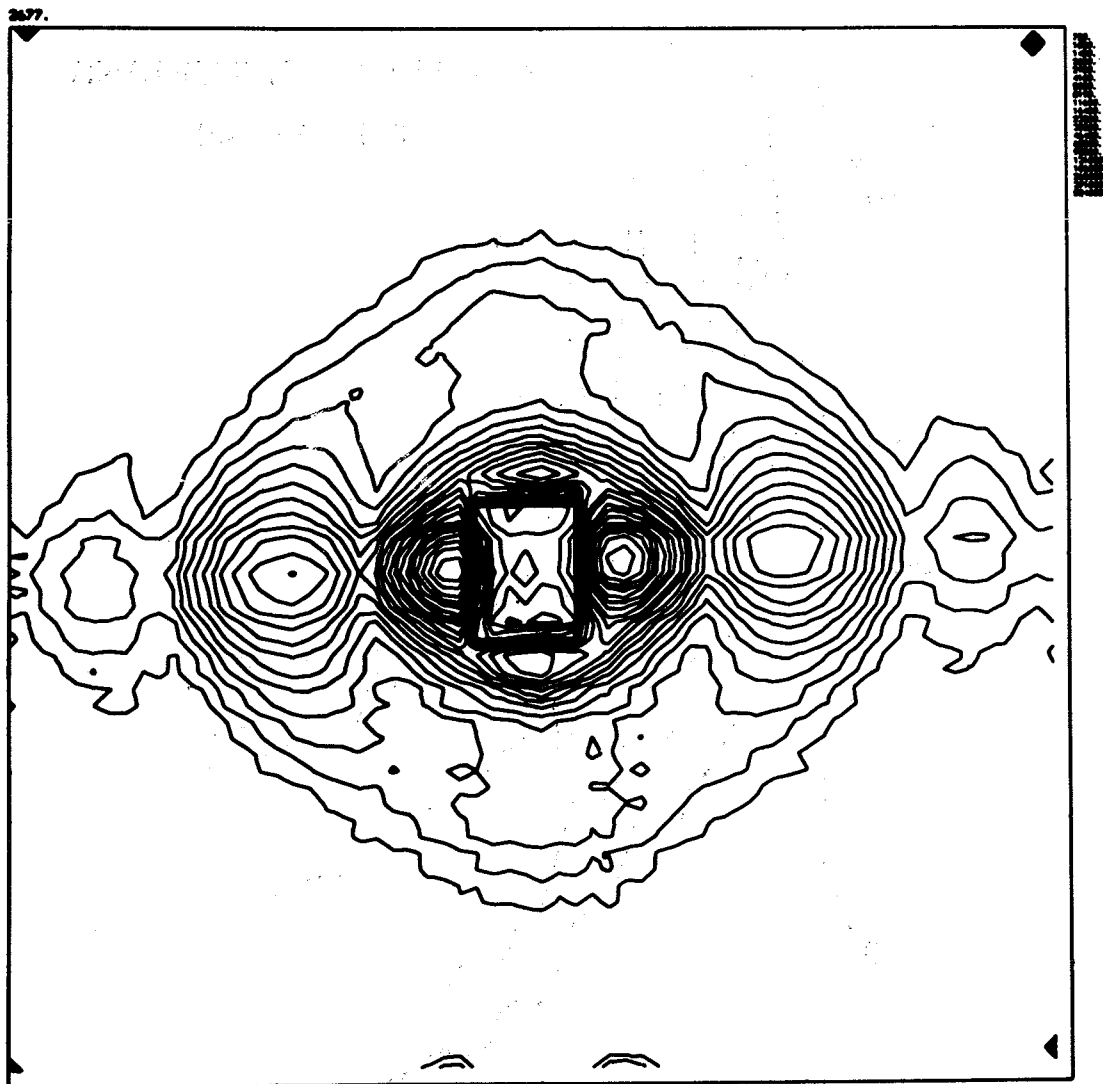


Fig. 11 Contour map of raw data: Diffraction pattern of an oriented gel of tobacco-mosaic virus.